

UNCLASSIFIED

AD NUMBER	
AD114950	
CLASSIFICATION CHANGES	
TO:	UNCLASSIFIED
FROM:	CONFIDENTIAL
LIMITATION CHANGES	
TO: Approved for public release; distribution is unlimited.	
FROM: Distribution: Further dissemination only as directed by Ballistic Research Lab., Aberdeen Proving Ground, MD, JUL 1956, or higher DoD authority.	
AUTHORITY	
USABRL ltr; Nov 28, 1980 ; ARL ltr., 28 July 2000	

THIS PAGE IS UNCLASSIFIED

UNCLASSIFIED

AD 114950

CLASSIFICATION CHANGED
TO: **UNCLASSIFIED**
FROM **CONFIDENTIAL**
AUTHORITY:

— BRL, PA 14, 28 Nov 80 —

produced From
Available Copy



UNCLASSIFIED

AD- 114950

SECURITY REMARKING REQUIREMENTS

DOD 5200.1-R, DEC 78

REVIEW ON 28 JUL 76

BRL

MEMORANDUM REPORT No. 1019

JULY 1956

Classified: *Unclassified*
By Authority of: *Comment No. 2, 10 K dts*
26 March 63 from CO. BRL
By: *[Signature]*
Security Officer (Officer)
Ballistic Research Laboratories
(Grade Orgn.)
Date: *14 Oct 63*

Air Blast Measurements Around Moving Explosive Charges, Part III (U)

B. F. ARMENDT

J. SPERRAZZA

Approved for public release;
distribution is unlimited

DEPARTMENT OF THE ARMY PROJECT No. 5B03-04-002
ORDNANCE RESEARCH AND DEVELOPMENT PROJECT No. TB3-0112

BALLISTIC RESEARCH LABORATORIES



ABERDEEN PROVING GROUND, MARYLAND

BALLISTIC RESEARCH LABORATORIES

MEMORANDUM REPORT NO. 1019

JULY 1956

AIR BLAST MEASUREMENTS AROUND MOVING EXPLOSIVE CHARGES, PART III (U)

B. F. Armendt
J. Sperrazza

Department of the Army Project No. 5B03-04-002
Ordnance Research and Development Project No. TB3-0112

ABERDEEN PROVING GROUND, MARYLAND

UNCLASSIFIED

TABLE OF CONTENTS

	Page
PREFACE	3
ABSTRACT	5
INTRODUCTION	7
EXPERIMENTAL PROCEDURE	8
DATA	14
THEORY	15
COMMENTS	20
REFERENCES	27
ADDENDUM	28
DISTRIBUTION LIST	31

PREFACE

This paper was originally presented at the Seventh AXP Tripartite Conference, U. S. Naval Ordnance Laboratory, White Oak, Maryland in April, 1956. Subsequently, D. J. Hinz of the Ballistic Research Laboratories has obtained additional data which appear to corroborate statements made in the paper. A brief discussion of his results is included as an Addendum.

Page intentionally blank

BALLISTIC RESEARCH LABORATORIES

MEMORANDUM REPORT NO. 1019

BFarmendt/JSperrazza/plg
Aberdeen Proving Ground, Md.
July 1956

AIR BLAST MEASUREMENTS AROUND MOVING EXPLOSIVE CHARGES, PART III (U)

ABSTRACT

Air blast measurements have been made around $3/8$ pound bare spherical charges detonated while moving at supersonic velocity. Experimental peak pressure data are presented and are compared to a theory based on the law of conservation of momentum. Agreement between the theory and experiment appears to be satisfactory. The conclusion, based on this theory, is that the velocity effect will probably be of more significance for relatively small charge weights, and/or at high altitudes.

Page intentionally blank

INTRODUCTION

Since most warheads containing high explosive are in motion at the instant of detonation, it is of interest to study the effect of this motion on the air blast produced by the weapon. This "velocity effect" was first noticed during aircraft vulnerability firings in the United States and Great Britain, and also during Swiss firing trials (1) of 20mm Oerlikon ammunition against box structures. It appeared that the detonating shells caused an increased amount of damage in the direction of motion, and a decreased amount in the opposite direction. Various explanations of the velocity effect have been advanced (2,3,4) but evaluation of these theories required quantitative data. Therefore, in 1952 experiments were begun at the Ballistic Research Laboratories for the purpose of providing these data. It was felt that the data could be obtained directly by

1. projecting an explosive at a desired terminal velocity,
2. detonating the explosive at a desired position in space, and
3. measuring the blast around the detonation.

Early work was performed by Patterson and Wenig (5), who, after great difficulty, succeeded in projecting a bare sphere of explosive at supersonic velocity and detonating it in flight, thus forming the basic experimental procedure which has since been used in all moving charge experiments at the Ballistic Research Laboratories. Unfortunately, the air blast data obtained at that time was only qualitative, because of the state of development of the instrumentation. The experiments were continued in 1954 by Armendt (6) with only minor modifications in procedure, and resulted in the collection of somewhat better data, but still insufficient to establish any rigorous theory. Further experiments have been conducted and have led to the establishment of a theory by which the behavior of the shock wave produced by the detonation of a moving charge may be explained in part.

EXPERIMENTAL PROCEDURE

Projection of the Charge

The first step in the construction of the moving charge experiments was to choose the type and size of charge and to find some means of projecting it at high velocity. Since even a light metal case on the charge produces fragments of a size and velocity sufficient to interfere with air blast measurements, it was decided to use a bare charge. Because of the symmetry of shock waves produced by spherical charges, a spherical shape was chosen. A number of devices for projecting the charge were suggested, but all were abandoned in favor of a conventional cannon. The caliber, and therefore the charge weight of $3/8$ pound, was dictated by the large surplus of 57mm guns. The rifling was bored out, resulting in a smoothbore gun of bore diameter 2.293 inches. Charges were made to fit this bore with a small clearance.

Having settled on the 57mm smoothbore gun and the $3/8$ pound bare spherical charge, the problem remained to project the charge from the gun. After a great deal of experimentation (5), Patterson succeeded in projecting $3/8$ pound, bare spheres of Composition B at a velocity of about 1700 to 1900 feet per second. For this, he used a propellant charge of 8 ounces of type 5316 powder confined in an M23-A2 57mm brass cartridge case, and a sabot consisting of 3 ounces of absorbent cotton in three separate wads. The main problem was charge breakup, which occurred on about 40% of the shots. More recent work by Armendt (7) resulted in a lower percentage of charge breakup, due to the substitution of fiberglass-reinforced Pentolite for the Composition B used by Patterson. The reinforced Pentolite has been utilized in all recent experimental work.

Detonation of the Charge

After the charges had been successfully projected from the gun, attention was turned to the problem of detonating the charges while in flight and at a desired position. A number of schemes were tried and the one finally settled upon is as follows. The charge is cast in a spherical form with a cylindrical well extending into the charge about $2/3$ of the

diameter. (See Figure 1.) In the bottom of the well is placed a tiny bit of Composition C-3 and an M-18 tetryl booster to insure high order detonation. Next comes an M-36 electric detonator. Across the leads of the detonator is placed a small coil made of number 28 copper wire wound on a short length of iron rod. All spaces are carefully packed with Composition C-3 to prevent the setback forces, experienced upon firing, from dislodging any part. The charges fused in this manner are fired from the gun through a screen wound with number 40 copper wire. The screen is placed just in front of a stationary coil consisting of three turns of number 4 copper wire approximately 7-1/2 inches in diameter. As the charge passes through the screen and into the stationary coil, the wire screen is broken, triggering an electronic circuit which causes a large condenser to be discharged through the stationary coil. The resulting "pulsed" magnetic field induces a current in the small coil inside the charge, which flows through the electric detonator and detonates the charge. If the orientation of the small coil is unfavorable, insufficient current may be induced and the charge may not fire.

Locating the Point of Detonation

Since the accuracy obtained with the smoothbore gun is not particularly good, and since the magnetic induction system of detonating the charge is not perfect, the point at which detonation occurs will rarely be exactly at the point desired. If the data are to be meaningful, it is necessary that the point of detonation be located fairly accurately. Therefore, two cameras equipped with 1-microsecond electronic shutters were placed 90 degrees apart and 10 feet from the desired point of detonation. When the charge detonates, a photocell device triggers the cameras, taking a picture of the luminous shock wave. By triangulation, the position of the charge at the instant of detonation can be located to within about 1/4 inch. A typical photograph of the detonating charge is shown in Figure 2.

Measurement of Charge Velocity

The velocity with which the charge is projected is measured as follows. After the charge leaves the muzzle of the gun and before it passes through the stationary coil where it is detonated, it passes through two wire screens wound with number 40 copper wire placed about 8 feet apart. Breakage of these

**SECTIONAL VIEW OF FUZED CHARGE
LOADED IN 57 mm SMOOTHBORE GUN
(NOT TO SCALE)**

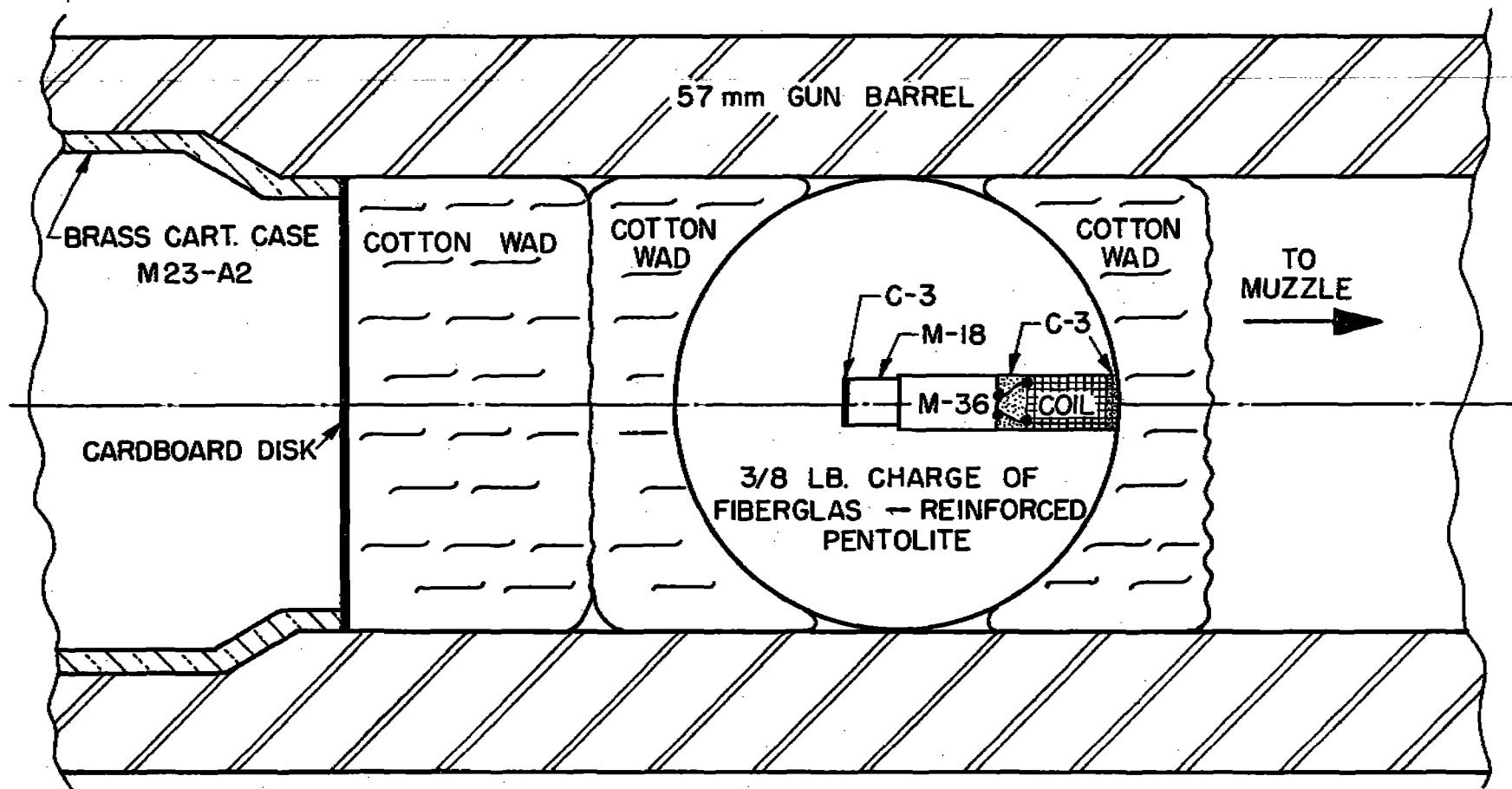




FIGURE 2

screens starts and stops an electronic counter chronograph, thus measuring the time necessary to traverse this interval. From this measurement, the average velocity over the interval can be calculated.

Air Blast Measurements

In the earlier work by Patterson and Wenig, and also by Armendt, the peak pressure and positive impulse of the shock wave produced by the detonation of the moving charge were measured by five pancake-type side-on pressure gages placed at different points around the detonating charge. It became evident, however, that more instrumentation would be required if useful data were to be obtained. Therefore, in recent experiments, a total of twelve side-on pressure gages, each spanned by a pair of face-on "velocity" gages, have been used. (See Figure 3.) The side-on gages were placed at a distance of 2.71 feet from the desired point of detonation, and at angles of 15° , 45° , 75° , 105° , 135° , and 165° from the direction of motion of the charge. The electrical output of each of these side-on gages was amplified and displayed on an oscilloscope. The face of the oscilloscope was photographed by a streak camera in which the 35mm film was moving approximately 1.25 inches per millisecond. Suitable timing marks were also recorded on the film, providing a time calibration.

When the charge detonates, the initial burst of light from the luminous shock wave is seen by a photocell device which triggers the cameras, as was previously mentioned. This same photocell device also starts twelve electronic counter chronographs. When the shock wave from the detonating charge reaches the first velocity gage at one of the twelve measuring positions, the chronograph corresponding to that position is stopped, giving a measure of the time of arrival, and a second counter chronograph is started. The shock wave sweeps past the first velocity gage, over the side-on pressure gage and finally reaches the rear velocity gage which stops the second counter chronograph. This second chronograph has now measured the time necessary for the shock to traverse the interval between the velocity gages, from which the average shock velocity over the interval can be calculated. Knowing the average shock velocity, the peak pressure at the center of the interval can be calculated by the Rankine-Hugoniot relation:

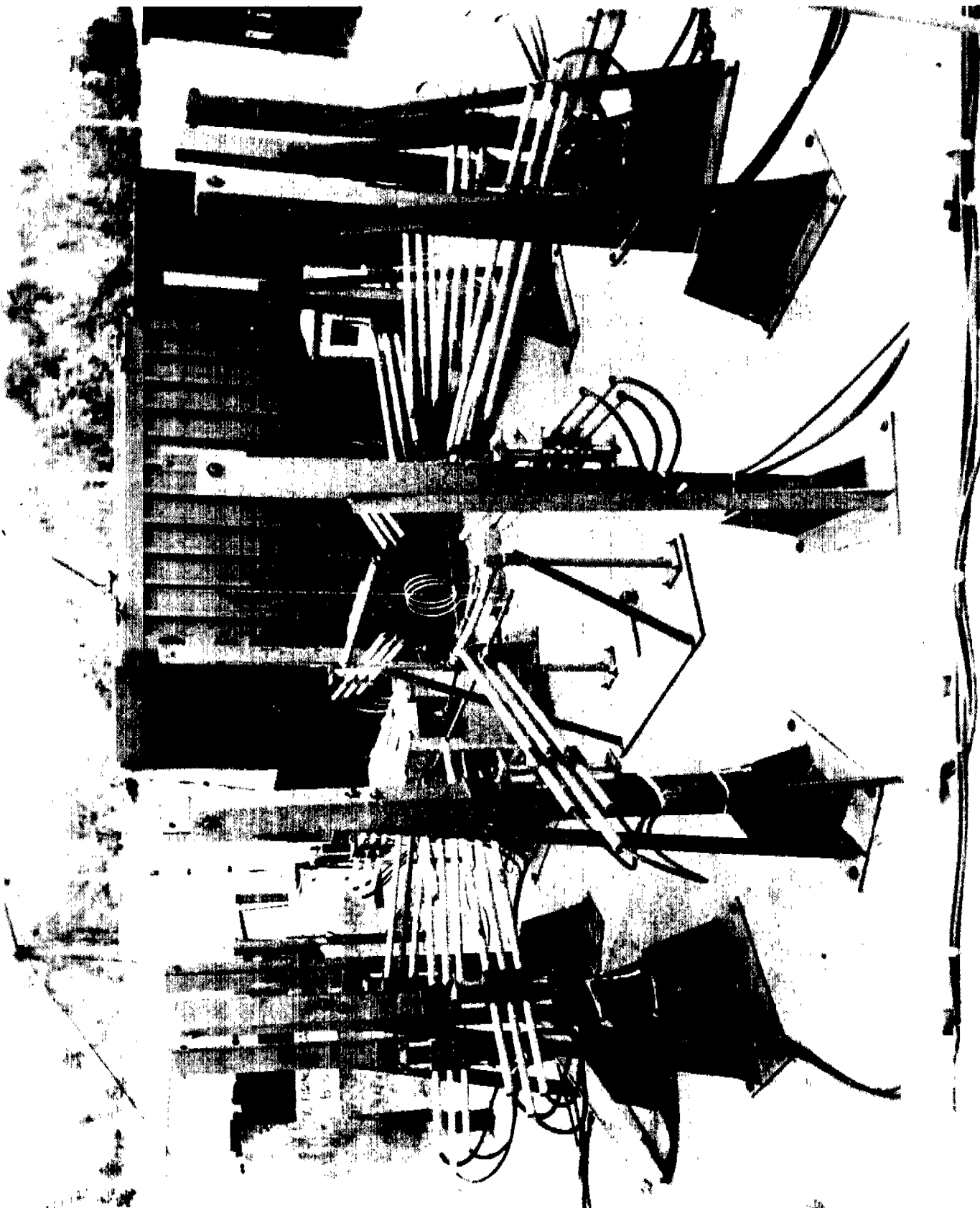


FIGURE 3

$$\frac{P_s}{P_o} = \frac{2\gamma}{\gamma + 1} \left(\frac{V^2}{C^2} - 1 \right)$$

where:

P_s = peak excess pressure

P_o = atmospheric pressure

γ = ratio of specific heats for air

V = shock velocity

C = sound velocity

Thus the 24 counter chronographs, 24 velocity gages, and the photocell device make up a system which can measure the shock arrival time, shock velocity, and peak excess pressure at twelve locations around the detonating charge.

DATA

Summaries of the experimental data reported in references 5 and 6 are repeated in Table I and II under appropriate labels. More recent data have been obtained with the experimental setup described above. For the purposes of discussion, these data are separated into two parts, the Time of Arrival Data and the Peak Pressure Data.

Time of Arrival Data

The time of arrival data which were obtained are shown in Table III. It was hoped that these data would tell whether the shock wave from a charge detonated while moving was distorted in any way, or remained spherical. The analysis of the data proceeded as follows: it was noticed that, for a given gage position, although the deviations in distance from the charge resulted in considerable variation in the measured time of arrival, the deviations in angle did not. Therefore, the angular deviations were neglected, and the nominal angles (i.e., 15° , 45° , etc.) were used. This approximation is considered satisfactory, and greatly simplifies the analysis.

Over the small intervals of distance involved, it was assumed that the shock velocity was constant, and therefore, linear least square fits were made to the time of arrival data. The equations for these least square lines are also shown in Table III. In order to determine the shape of the shock wave, these equations were solved for R (distance from the charge)

using values of t_a (time of arrival) equal to 400, 550, and 700 microseconds. The results are plotted in Figure 4.

It appeared that the points fell on a circle whose center was shifted in the direction of motion of the charge. Because of the significance of this result, it was carefully checked by both analytical and graphical methods, but the answer was the same. Therefore, it can be said that, within the experimental error, the shock wave produced by the detonation of a moving, spherical charge remains spherical, but that the center of the sphere moves in the direction of motion of the charge prior to detonation.

Peak Pressure Data

The peak pressure data obtained from seven rounds are shown in Table IV, under "Experimental Data for Moving Charges." The mean velocity of the seven rounds was 1760 feet/second.

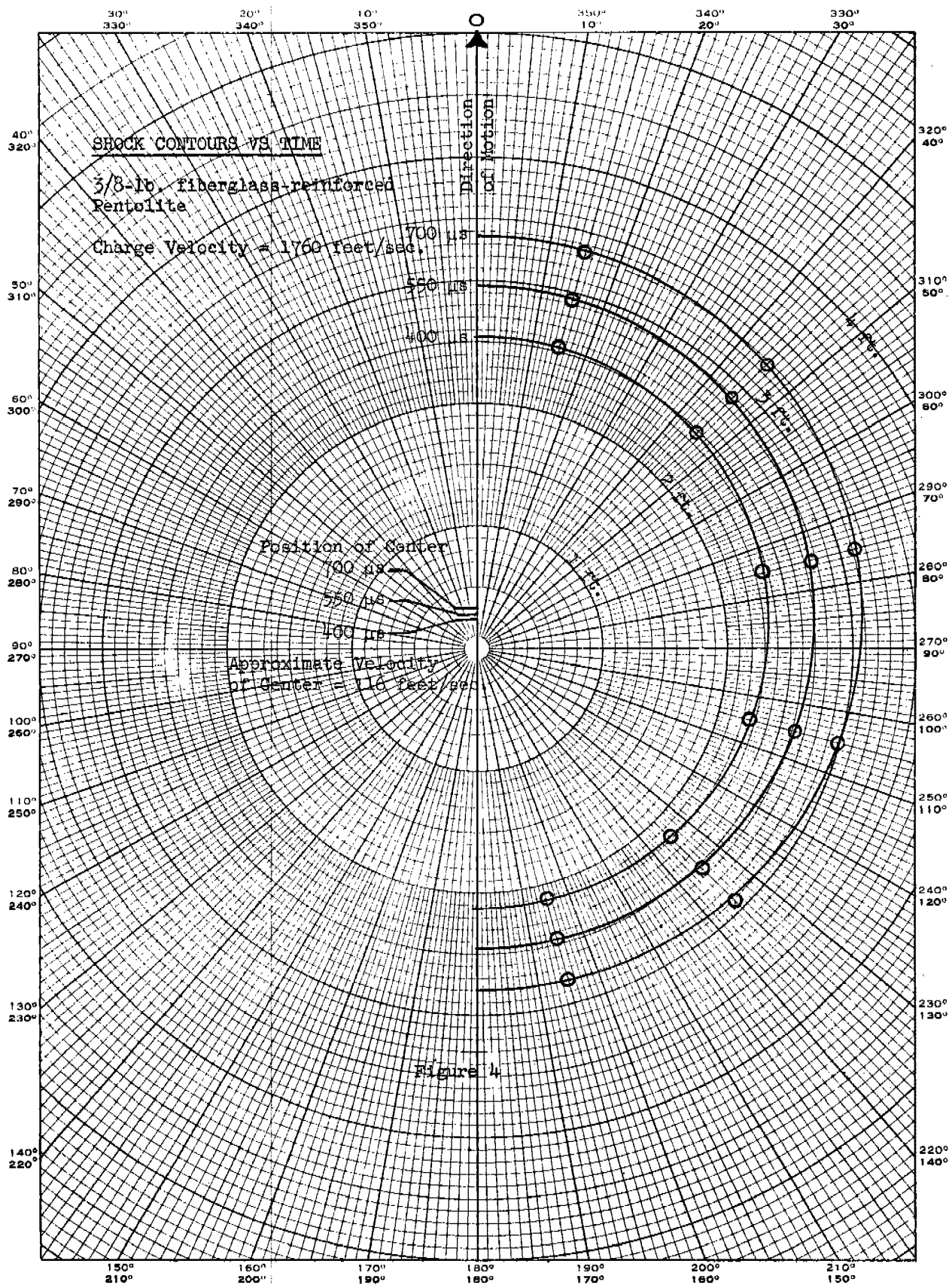
The positive impulse data obtained in the recent firings have not yet been reduced, and therefore, no additional data on positive impulse will be presented at this time.

THEORY

Thornhill and Hetherington (3) predicted that, close to the surface of a moving charge, the shock velocity, and thus inference of the peak pressure, could be approximated by vectorial addition of the shock velocity for the stationary charge and the terminal velocity of the moving charge. Time of arrival measurements, discussed above, indicate that the same rule is applicable to the expanded shock wave, if the velocity of the center is substituted for the terminal velocity of the charge.

Since the radial velocity of shock waves from stationary charges has been measured, it is seen that the position and velocity of the shock front could be described if the velocity of the center of the shock were known as a function of time.

The velocity of the center of the shock wave at any time can be predicted by application of the principle of conservation of linear momentum. Thus the momentum of the explosive prior to detonation is set equal to the momentum of the explosion gases and air contained by the spherical shock, it



being assumed that the average velocity of all the contained gases and air is that of the center of the sphere.

Let

- M_e = weight of explosive (lbs)
- M_a = weight of air contained by the spherical shock (lbs)
- V_o = terminal velocity of the explosive (ft/sec)
- V_c = velocity of center of shock wave (ft/sec)
- d = radius of spherical shock wave (feet)
- r = radius of spherical shock wave (charge radii)
- a = charge radius (feet)
- ρ_a = density of air (lbs/ft³)
- ρ_e = density of explosive (lbs/ft³)

Neglecting the mass of air displaced by the explosive charge, application of the law of conservation of linear momentum gives:

$$M_e V_o = (M_e + M_a) V_c = (M_e + \frac{4}{3} \pi \rho_a d^3) V_c \quad (1)$$

or

$$V_c = \frac{M_e V_o}{M_e + \frac{4}{3} \pi \rho_a d^3} \quad (1a)$$

Since

$$M_e = \frac{4}{3} \pi \rho_e a^3 \quad (2)$$

Equation (1a) reduces to:

$$V_c = \frac{V_o}{1 + \frac{\rho_a}{\rho_e} r^3} \quad (3)$$

Therefore, at a time when the radius of the shock wave is equal to r , the velocity of the center of the shock wave is given by equation (3). The distance that the center has traveled (in the direction of original charge motion) from the point of detonation at any time t is:

$$r_c = \int_0^t V_c dt. \quad (4)$$

Referred to a stationary frame the shock velocity on the surface of the spherical shock wave produced by the moving charge becomes (see Figure 5):

$$\vec{U}_m = \vec{U}_s + \vec{V}_c$$

Where:

\vec{U}_m = shock velocity at distance r and angle from line of flight ϕ for moving charge.

\vec{U}_s = shock velocity at distance r for stationary charge.

ϕ = angle from line of flight (referred to center of shock wave).

Once the shock velocity is known, the peak pressure can be found.

Ordinarily, the distance r and angle ϕ from the center of the shock wave are not known, measurements being made from the point of detonation. (See Figure 6.) Therefore, the quantities known are R and θ , and, by integration, r_c . The distance and angle from the shock center can be found by:

$$R = r_c \cos \theta + (r^2 - r_c^2 \sin^2 \theta)^{1/2} \quad (5)$$

$$\sin \phi = \frac{R}{r} \sin \theta$$

Thus far, no simple scheme has been found for scaling the various parameters associated with the velocity effect, such as altitude, charge weight, charge velocity, etc. Therefore, rather lengthy computation is necessary to obtain theoretical values of the peak pressure at various points around a given point of detonation, since each case must be considered individually. These calculations have been made for the conditions obtaining for all of the experimental peak pressure data shown in Table IV. The results are shown in Table IV under "Calculated Data for Moving Charges."

For the purpose of comparing the theory with the experiments, the ratios of the theoretical peak pressures to the experimental peak pressures have been taken, and are also shown in Table IV. The mean value of the ratios is .991 with a standard deviation of the individual of 11.5%. Examination of these ratios has disclosed no systematic error, and it is concluded that the theory adequately approximates the experimental results.

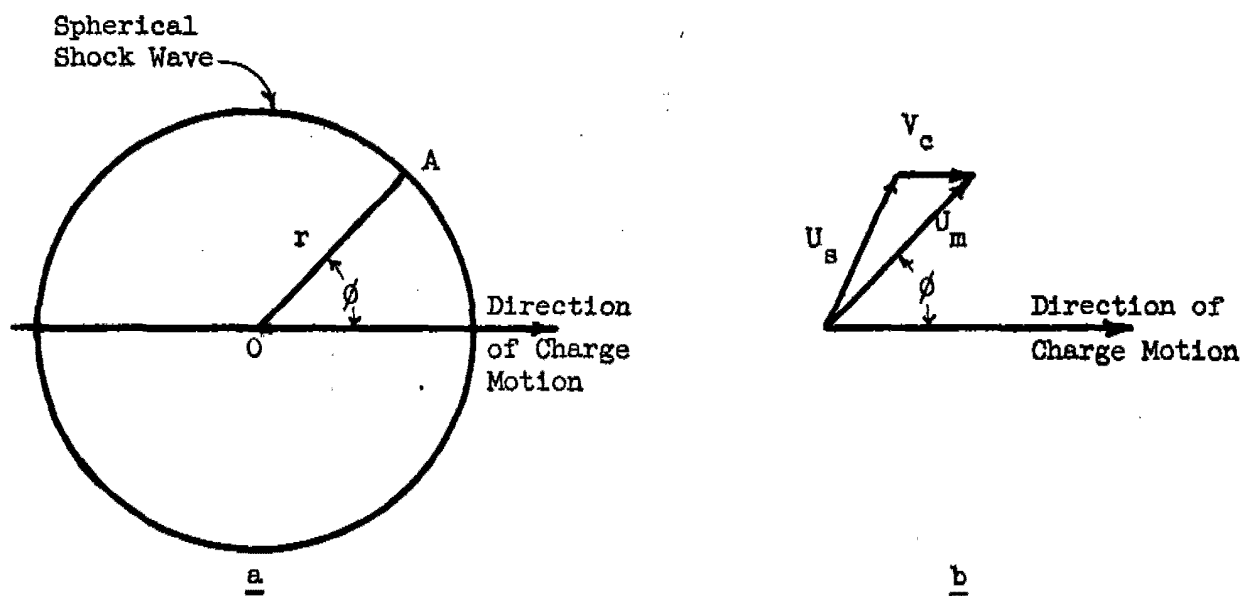


Figure 5

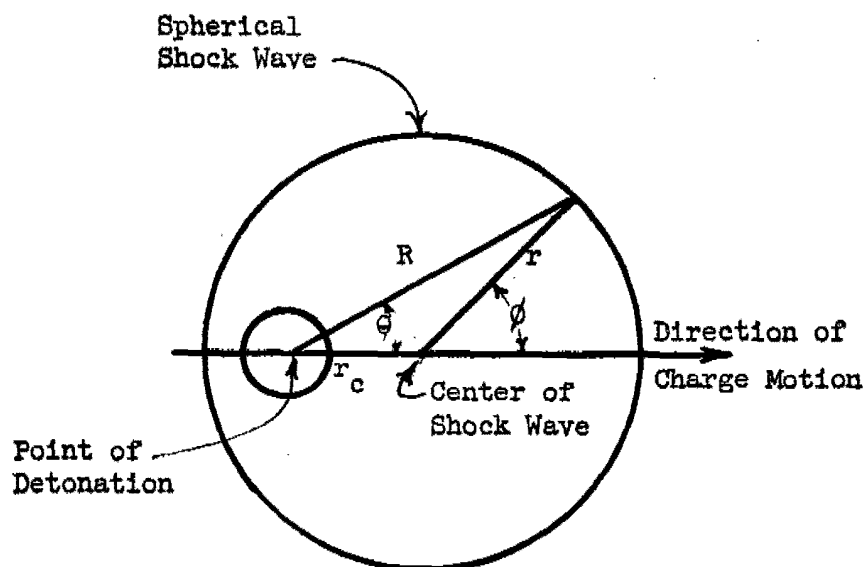


Figure 6

The positive impulse in the shock wave from a moving charge is known to be enhanced in the direction of charge motion (see Tables I and II), but no simple scheme for prediction of the enhancement has been suggested. It is hoped that recently obtained data, now in the process of being reduced, will throw some light on the subject.

COMMENTS

The conclusion is that the theory advanced appears to predict the effect of charge motion on the peak pressure in the shock wave produced when a moving spherical charge is detonated. Furthermore, if this theory is correct, it is seen that the velocity effect would be of greater significance for relatively small charges. With nuclear warheads, for example, the velocity effect would be of little consequence, since at the peak pressure levels where the velocity effect might cause some enhancement of damage, the mass of air contained by the shock wave would far outweigh the original warhead. Only if the weapon were detonated outside the atmosphere and/or if the warhead were moving at very high velocities would the velocity effect be even measurable.

A great deal of work remains to be done before the velocity effect can be completely understood. As previously mentioned, the behavior of the positive impulse requires explanation. Before the peak pressure theory described above can be considered as established, further experiments utilizing higher charge velocities and greater charge weights are necessary. High altitude experiments are especially desirable, since it is expected that the velocity effect will be of much greater significance for low atmospheric pressures. In addition, the effect of a metal casing on the velocity effect must be investigated, since warheads are ordinarily cased.

B. F. Armendt

B. F. ARMENDT

J. Sperrazza
J. SPERRAZZA

TABLE I

SUMMARY OF EXPERIMENTAL DATA FROM BRLM 767

2.36 feet from a 3/8 pound bare, spherical Composition B charge

Charge Velocity	0 ft/sec	1982 ft/sec		
		Angle from Line of Flight		
		15°	45°	105°
Peak Pressure (psi)	73	109	87	55
Positive Impulse (psi-ms)	7.8	14.4	13.0	7.0

TABLE II

SUMMARY OF EXPERIMENTAL DATA FROM BRLM 900

2.71 feet from a 3/8 pound bare, spherical Composition B charge

Charge Velocity	0 ft/sec	1753 ft/sec		
		Angle from Line of Flight		
		15°	45°	105°
Peak Pressure (psi)	67.3	91.0	82.0	52.5
Positive Impulse (psi-ms)	8.1	10.2	9.8	7.9

TABLE III
TIME OF ARRIVAL DATA

Type of charge - 3/8 pound bare, spherical charges of fiberglass-reinforced Pentolite

Mean velocity of charges - 1760 feet/second

Nominal angle from line of flight = 15°

Round No.	Distance from Charge (feet)	Arrival Time (μ s)	Distance from Charge (feet)	Arrival Time (μ s)
534	2.66	468.8	3.16	628.8
	2.71	480.6	3.21	663.1
578	2.69	443.1	3.19	635.6
	2.69	452.5	3.19	624.4
582	2.56	419.4	3.06	585.7
587	2.45	382.5	2.95	563.8
588	2.73	468.1	-	-
590	2.53	383.1	3.03	556.9
	2.58	428.1	3.08	606.2

Least square fit:

$$t_a = 517.1 + 388.2 (R - 2.846)$$

t_a = time of arrival (μ s)

R = distance from charge (feet)

Nominal angle from line of flight = 45°

Round No.	Distance from Charge (feet)	Arrival Time (μ s)	Distance from Charge (feet)	Arrival Time (μ s)
534	2.69	478.1	3.19	686.2
549	2.80	470.0	3.30	701.3
578	2.62	477.5	3.12	676.3
582	2.50	402.5	3.00	584.4
587	2.49	415.0	2.99	598.1
	2.43	388.1	2.93	566.9
590	2.59	438.8	3.09	621.3

Least square fit:

$$t_a = 536.0 + 378.7(R - 2.837)$$

TABLE III (continued)

Nominal angle from line of flight = 75°

Round No.	Distance from Charge (feet)	Arrival Time (μ s)	Distance from Charge (feet)	Arrival Time (μ s)
534	2.62	533.1	3.12	748.7
549	2.37	406.9	2.87	573.8
	2.59	530.6	3.09	731.2
578	2.52	465.0	3.02	643.1
	2.54	440.0	3.04	661.3
582	2.45	433.1	2.95	621.9
	2.52	466.3	3.02	668.2
587	2.50	457.5	3.00	655.0
	2.42	421.3	2.92	623.2
588	2.69	516.9	3.19	707.5
	2.37	419.4	2.87	591.3
590	2.40	390.6	2.90	581.9
	2.57	478.8	3.07	676.9

Least square fit:

$$t_a = 555.5 + 398.5 (R - 2.755)$$

Nominal angle from line of flight = 105°

Round No.	Distance from Charge (feet)	Arrival Time (μ s)	Distance from Charge (feet)	Arrival Time (μ s)
549	2.59	530.0	3.09	747.5
578	2.40	447.5	2.90	653.8
	2.42	475.6	-	-
582	2.47	500.0	-	-
587	2.50	501.3	3.00	714.4
	2.42	471.9	2.92	696.3
588	2.58	497.5	3.08	708.1
	2.24	417.5	2.74	611.3
590	2.35	447.5	-	-
	2.52	510.6	3.02	726.2

Least square fit:

$$t_a = 568.1 + 403.6 (R - 2.662)$$

TABLE III (continued)

Nominal angle from line of flight = 135°

Round No.	Distance from Charge (feet)	Arrival Time (μ s)	Distance from Charge (feet)	Arrival Time (μ s)
549	2.13	387.5	-	-
578	2.31	466.9	-	-
582	2.37	467.5	2.87	693.8
	2.42	511.2	-	-
587	2.43	505.0	-	-
588	2.43	475.0	-	-
	2.18	415.0	-	-
590	2.46	507.5	-	-

Least square fit:

$$t_a = 492.2 + 399.9 (R - 2.399)$$

Nominal angle from line of flight = 165°

Round No.	Distance from Charge (feet)	Arrival Time (μ s)	Distance from Charge (feet)	Arrival Time (μ s)
534	2.27	440.0	2.77	653.8
549	2.25	452.5	2.75	643.1
578	2.23	467.5	2.73	673.8
	2.24	476.3	-	-
582	2.37	535.0	2.87	756.9
	2.39	530.0	-	-
587	2.48	560.0	2.98	791.3
	2.45	538.1	-	-
588	2.29	474.4	2.79	676.3
	2.19	439.4	-	-
590	2.35	493.8	2.85	734.4
	2.40	527.5	-	-

Least square fit:

$$t_a = 571.8 + 431.7 (R - 2.506)$$

TABLE IV

EXPERIMENTAL DATA FOR MOVING CHARGES

Type of charge - 3/8 pound bare sphere of fiberglass-reinforced Pentolite
Mean velocity of charge - 1760 feet/second

Rd. No.	Atmospheric Temperature (°F)	Atmospheric Pressure (in Hg)	Angle from Line of Flight (degrees)	Distance from Charge (feet)	Shock Velocity (ft/sec)	Peak Pressure (lb/in ²)
534	52	29.80	12.0 69.8 161.5 71.1 43.2 15.7	2.91 2.69 2.52 2.87 2.94 2.96	3125 2389 2389 2319 2403 2740	118.3 62.0 58.7 57.5 62.9 87.0
549	74	29.83	10.0 38.1 57.9 159.1 98.4 70.7 43.7	2.95 2.80 2.62 2.50 2.84 2.98 3.07	2614 2847 2996 2623 2299 2493 2162	73.9 90.9 102.4 74.6 53.3 65.7 45.1
576	70	30.12	13.6 41.5 70.2 100.1 131.4 163.8 70.4 41.9 14.0	2.94 2.87 2.77 2.65 2.54 2.48 2.79 2.89 2.94	2597 2515 2807 2424 2347 2424 2259 2128 2909	74.1 68.4 89.5 62.3 70.6 62.3 51.9 44.1 97.3
582	75.5	30.11	13.8 43.2 73.0 103.4 134.2 165.3 73.4 44.3 15.3	2.79 2.75 2.70 2.65 2.62 2.62 2.77 2.80 2.81	3041 2749 2648 2405 2210 2253 2477 2469 3007	106.7 84.0 76.7 60.1 48.2 50.8 64.9 64.4 103.9
587	78	30.05	15.9 45.7 75.3 104.8 164.1 105.3 74.8 44.4 14.1	2.72 2.74 2.75 2.75 2.73 2.67 2.67 2.68 2.70	2817 2731 2532 2346 2162 2228 2477 2796 2758	88.3 82.0 66.0 56.0 44.9 48.8 64.4 86.8 83.9

CALCULATED DATA FOR MOVING CHARGES

Distance from Charge (charge radii)	r (charge radii)	r _c (charge radii)	θ (degrees)	Center Velocity (V _c) (Mach No.)	Radial Shock Velocity (Mach No.)	Theoretical Peak Pressure (psi)
30.4584 28.1034 26.3764 30.0502 30.7934 30.9504	27.8805 27.3087 26.9394 29.2685 28.8957 28.3945	2.6438 2.6203 2.6855 2.6990 2.6840 2.6647	13.09 74.90 163.18 76.12 46.85 17.16	.0917 .0971 .0825 .0797 .0829 .0870	2.2385 2.2951 2.1452 2.1220 2.1526 2.1918	75.25 74.40 55.66 61.02 66.05 71.07
30.8457 29.2757 27.4335 26.1461 29.7153 31.1493 31.8819	28.2828 27.3030 26.5239 26.6076 29.7153 30.3657 30.0089	2.6061 2.5657 2.5344 2.6186 2.6787 2.6837 2.6710	10.91 41.43 72.95 160.97 103.52 75.42 47.28	.0878 .0970 .1046 .0851 .0728 0.719 .0743	2.2007 2.2957 2.3667 2.1752 2.0541 2.0443 2.0692	57.16 68.39 80.87 57.71 53.70 55.45 59.51
30.7306 30.0816 28.9931 27.7161 26.5857 25.9577 29.2234 30.2386 30.7934	28.1671 28.1563 28.2078 28.3022 26.4107 28.5207 28.4420 28.3196 28.2386	2.6441 2.6437 2.6458 2.6497 2.6539 2.6581 2.6551 2.6503 2.6468	14.84 45.08 75.27 155.40 135.42 165.33 75.43 45.43 15.32	.0895 .0896 .0891 .0882 .0873 .0864 .0871 .0861 .0851	2.2117 2.2127 2.2078 2.0890 2.1905 2.1820 2.1881 2.1977 2.2054	73.64 71.92 68.40 56.92 60.73 58.52 66.81 70.64 73.06
29.1806 28.7628 28.2499 27.7685 27.4440 29.3390 27.3812 28.9826 29.2862 29.3594	26.7151 26.5653 27.6094 28.4817 28.4440 29.9549 28.3528 27.5110 28.2862 26.9220	2.5261 2.5362 2.5633 2.5963 2.6310 2.6532 2.6532 2.5933 2.5593 2.5348	15.10 46.88 78.10 108.49 137.89 166.55 78.44 47.97 16.67	.0882 .0892 .0932 .0854 .0785 .0740 .0864 .0941 .1000	2.3533 2.3274 2.2646 2.1250 2.1180 2.0730 2.1951 2.2739 2.3321	66.22 61.46 72.50 62.90 55.78 51.58 66.97 76.74 84.19
28.4593 28.6686 28.8047 28.6241 28.8256 28.5221 27.9559 27.9150 28.0092 28.2185	26.0373 26.9376 26.2534 26.6241 28.8256 31.1581 28.7473 27.9150 26.2533 25.7852	2.5286 2.5664 2.6242 2.6769 2.7316 2.7316 2.6433 2.5865 2.5382 2.5162	17.44 49.62 80.46 109.25 165.50 165.50 110.40 80.07 48.25 15.46	.1123 .1022 .0892 .0781 .0679 .0679 .0852 .0979 .1096 .1154	2.4276 2.3301 2.2035 2.0961 1.9599 2.1642 2.2891 2.4094 2.4572	95.12 81.42 67.30 56.36 46.40 61.07 74.10 87.65 96.06

COMPARISON

Ratio of	Calc. peak pressure	Exp. peak pressure
	.636	1.230
	.648	1.062
	.648	1.049
	.617	1.049
	.773	1.318
	.882	1.051
	.790	1.051
	.774	1.051
	1.008	1.051
	.545	1.051
	1.318	1.051
	.994	1.051
	.970	1.051
	.945	1.051
	.913	1.051
	.860	1.051
	.929	1.051
	1.288	1.051
	1.603	1.051
	.751	1.051
	.808	1.051
	.970	1.051
	.945	1.051
	1.047	1.051
	1.158	1.051
	1.016	1.051
	1.032	1.051
	1.191	1.051
	.611	1.051
	1.054	1.051
	.994	1.051
	.989	1.051
	1.006	1.051
	1.033	1.051
	1.251	1.051
	1.152	1.051
	1.012	1.051
	1.145	1.051

TABLE IV (Cont.)

EXPERIMENTAL DATA FOR MOVING CHARGES

Rd. No.	Atmospheric Temperature (°F)	Atmospheric Pressure (in Hg)	Angle from Line of Flight (degrees)	Distance from Charge (feet)	Shock Velocity (ft/sec)	Peak Pressure (lb/in ²)
568	83.5	30.05	71.5	2.94	2623	73.3
			99.6	2.83	2774	57.0
			160.0	2.54	2477	63.5
			100.8	2.49	2560	70.4
			69.1	2.62	2909	94.1
590	82	30.04	12.8	2.78	2877	92.1
			72.6	2.65	2614	73.0
			166.3	2.60	2078	39.8
			102.7	2.77	2319	53.8
			73.6	2.82	2524	66.9
			44.9	2.84	2740	81.9
			16.2	2.83	2807	86.8

CALCULATED DATA FOR MOVING CHARGES

Distance from Charge (charge radii)	r (charge radii)	r _c (charge radii)	φ (degrees)	Center Velocity (V _c) (Mach No.)	Radial Shock Velocity (Mach No.)	Theoretical Peak Pressure (psi)
30.7725	30.0217	2.7106	76.40	.0757	2.0663	57.52
29.5897	30.1593	2.7156	104.66	.0747	2.0587	54.27
26.5857	29.1145	2.6765	161.76	.0825	2.1355	55.48
26.0938	26.6982	2.5761	106.26	.1053	2.3550	75.66
27.4440	26.6357	2.5733	74.29	.1060	2.3614	60.68
29.0978	26.5954	2.5723	14.00	.1063	2.3655	87.42
27.7685	27.1042	2.5950	77.82	.1007	2.3135	76.38
27.1928	29.8270	2.7044	167.53	.0770	2.0839	51.92
29.0036	29.7123	2.7003	107.75	.0778	2.0900	56.11
29.5164	28.8774	2.6681	78.65	.0845	2.1541	65.70
29.6944	27.8936	2.6285	45.70	.0931	2.2374	73.50
29.5688	27.0872	2.5943	17.73	.1009	2.3153	82.61

COMPARISON

Ratio of	Calc. peak pressure	Exp. peak pressure
	.764	
	.953	
	.874	
	1.075	
	.859	
	.950	
	1.047	
	1.305	
	1.043	
	.952	
	.898	
	.951	

Mean .991
Standard deviation .114 = 11.5%

r = radius of spherical shock wave.
r_c = distance that center of shock wave has traveled from point of detonation.
φ = angle from line of flight with reference to the center of the shock wave instead of the point of detonation.

REFERENCES

1. Oerlikon Machine Tool Works, Zurich-Oerlikon, Switzerland Brochure No. 950, "Target-Velocity and Blasting Effect of 'Oerlikon' 20mm Ammunition."
2. NOL Memorandum No. 10983, "Charge Velocity and Blast Effect - Comments on Oerlikon Report," H. G. Snay, 1 July 1950.
3. ARE Memo 6153, "Some Notes on Explosions of Moving Charges," C. K. Thornhill and R. Hetherington, April 1953.
4. Rand Report RM-848, "Note on Directional Effect of Pressure Field of Moving Blast," J. D. Cole, 9 June 1952.
5. BRL Memorandum Report No. 767, "Air Blast Measurements Around Moving Explosive Charges," J. D. Patterson and J. Wenig, March 1954.
6. BRL Memorandum Report No. 900, "Air Blast Measurements Around Moving Explosive Charges, Part II," B. F. Armendt, Jr., May 1955.
7. BRL Memorandum Report No. 977, "Qualitative Tests of Dynamic Strength of Various Plastic-Bonded and Fiber-Reinforced Explosives," B. F. Armendt, Jr., February 1956.

[REDACTED]

ADDENDUM

In the section on "Time of Arrival Data," page 14, the statement was made that the shock wave produced by the detonation of a moving spherical charge remains spherical, but the center of the sphere moves in the direction of motion of the charge prior to detonation. This statement was supported by experimental data obtained with twenty-four time-of-arrival gages. Assuming that the statement is correct, a simple mathematical analysis was made (see the section on "Theory" page 15.) Such a simple construction would not be possible if the shock wave produced by the moving charge were distorted (i.e., not spherical).

Since the original paper was presented at the Seventh AXP Tripartite Conference, additional information has been obtained by D. J. Hinz, of the Ballistic Research Laboratories, using a photographic method. A spherical charge of fiberglass-reinforced Pentolite was projected at approximately 1800 feet per second and detonated in flight as described under "Experimental Procedure," page 8. The detonating charge was backlighted by means of an exploding wire placed at the focus of a 10-foot parabolic reflector. A camera facing in a direction normal to the line of flight and having a one-microsecond electronic shutter was synchronized with the exploding wire, and photographed the expanding shock wave. A sample photograph is shown in Figure 7, in which the shock wave has reached a diameter of approximately 58 inches. Close examination of the shock contour indicates that the shape is either spherical, or very close to it. This information substantiates the statement made in the original paper that the shock wave remains spherical.

The use of the above data, prior to publication by Mr. Hinz, is gratefully acknowledged.

Direction of
Charge Motion

Shock Front

Shock Front

FIGURE 7

Page intentionally blank

Page intentionally blank

Page intentionally blank

DISTRIBUTION LIST

<u>No. of Copies</u>	<u>Organization</u>	<u>No. of Copies</u>	<u>Organization</u>
	Chief of Ordnance Department of the Army Washington 25, D. C. Attn: ORDTB - Bal Sec ORDTA ORDTU ORDTX-AR	1	Chief of Naval Operations Department of the Navy Washington 25, D. C. Attn: Op 374 - Dr. J. Steinhardt
10	British Joint Services Mission 1800 K Street, NW Washington 6, D. C. Attn: Mr. John Izzard, Reports Officer Of Interest To: Mr. G. Simm, R.A.E.	1	Commanding Officer Naval Ordnance Laboratory Corona, California Attn: Dr. H. A. Thomas
4	Canadian Army Staff 2450 Massachusetts Avenue Washington 8, D. C.	5	Chief of Staff U. S. Air Force Washington 25, D. C. Attn: AFDRD-AC 2 cys DCS/O - Operations Analysis Division AFDRQ
3	Chief, Bureau of Ordnance Department of the Navy Washington 25, D. C. Attn: ReO	2	Director Air University Maxwell Air Force Base, Alabama Attn: AUL-5946
2	Commander Naval Proving Ground Dahlgren, Virginia	1	Director of Research & Development U. S. Air Force Washington 25, D. C. Attn: Armament Division (AFRDR-AR/1)
2	Commander Naval Ordnance Laboratory White Oak Silver Spring 19, Md.	3	Commander Wright Air Development Center Wright-Patterson Air Force Base, Ohio Attn: WCLGR-R WCLDI WCLSS-1
1	Commander Naval Ordnance Test Station China Lake, California Attn: Technical Library	1	Commander Air Technical Intelligence Center Wright-Patterson Air Force Base Ohio Attn: Associated Equipment Section, ATIAS
1	Commander Naval Air Development Center Johnsville, Pennsylvania	1	Director, Project RAND Department of the Air Force 1700 Main Street Santa Monica, California
9	Chief, Bureau of Aeronautics Department of the Navy Washington 25, D. C. Attn: Armament Division- 2 cys Research Division 1 cy Design Elements Div. 1 cy Evaluation Div. 1 cy Military Requirements Div. 1 cy Aircraft Division 1 cy Power Plant Div. 1 cy		

DISTRIBUTION LIST

<u>No. of Copies</u>	<u>Organization</u>	<u>No. of Copies</u>	<u>Organization</u>
1	Commander Air Proving Ground Eglin Air Force Base, Fla. Attn: Director of Armament	1	Director National Advisory Committee for Aeronautics 1512 H Street, NW Washington 25, D. C. Attn: Chief, Office of Aeronautical Intelligence
1	Commander Air Force Armament Center Eglin Air Force Base, Fla. Attn: ACOTT ACB	1	Director Weapon Systems Evaluation Group Office, Secretary of Defense The Pentagon Washington 25, D. C.
1	Commander Continental Air Command Mitchell Air Force Base New York	3	Commanding General Picatinny Arsenal Dover, New Jersey Attn: Samuel Feltman Ammunition Labs.
1	Commander Air Defense Command Ent Air Force Base, Colorado	1	Commanding General Frankford Arsenal Philadelphia 37; Pennsylvania Attn: Reports Group
3	Commander Strategic Air Command Offutt Air Force Base Omaha, Nebraska	1	President CONARC Board No. 4 Fort Bliss, Texas
1	Commander Tactical Air Command Langley Air Force Base Langley Field, Virginia	1	Commandant Antiaircraft & Guided Missile Center Fort Bliss, Texas
1	Commander Air Research & Development Command P. O. Box 1395 Baltimore 3, Maryland Attn: RDTAG	1	Army Ordnance Representative U. S. Naval Ordnance Test Station NOTS Annex 3202 E. Foothill Blvd. Pasadena 8, California
5	Director Armed Services Technical Information Agency Documents Service Center Knott Building Dayton 2, Ohio Attn: DSC-SD	2	Director Operations Research Office 7100 Connecticut Avenue Chevy Chase, Maryland Washington 15, D. C.

DISTRIBUTION LIST

<u>No. of Copies</u>	<u>Organization</u>	<u>No. of Copies</u>	<u>Organization</u>
1	Applied Physics Laboratory Johns Hopkins University 8621 Georgia Avenue Silver Spring, Maryland THRU: Naval Inspector of Ordnance Applied Physics Laboratory Johns Hopkins University Silver Spring, Maryland	1	Chance-Vought Aircraft, Inc. P. O. Box 5907 Dallas, Texas Attn: Dr. C. C. Wan THRU: Bureau of Aeronautics Rep. Naval Industrial Reserve Plant Aeronautics P. O. Box 5907 Dallas, Texas
1	Aerojet-General Corporation Azusa, California THRU: District Chief Los Angeles Ordnance District 55 South Grand Avenue Pasadena 2, California	1	Cornell Aeronautical Laboratory, Inc. 4455 Genesee Street Buffalo 21, New York THRU: Bureau of Aeronautics Rep. Cornell Aeronautical Lab, Inc. P. O. Box 235 Buffalo 21, New York
1	Boeing Airplane Company Wichita, Kansas Attn: Mr. W. A. Pearce THRU: Air Force Plant Representative Boeing Airplane Company Wichita, Kansas	1	Denver Research Institute University of Denver Denver 10, Colorado THRU: Office Naval Research Rep. University of Kansas Lawrence, Kansas
1	Boeing Airplane Company Seattle 14, Washington Attn: Mr. J. Christian, Armament Unit THRU: Air Force Plant Representative Boeing Airplane Company Seattle, Washington	1	Douglas Aviation Corporation Long Beach, California Attn: Mr. K. Kotter THRU: Air Force Plant Rep. Douglas Aircraft Corporation 3855 Lakewood Blvd. P. O. Box 200 Long Beach 1, California
1	CONVAIR Division of General Dynamics Corporation P. O. Box 1950 San Diego 12, California Attn: Mr. A. Bernstein, Chief, Systems Analysis	1	Director of Statistical Laboratory Purdue University Lafayette, Indiana Attn: Dr. Kossach THRU: District Chief Chicago Ordnance District 209 W. Jackson Blvd. Chicago 6, Illinois
1	CONVAIR Division of General Dynamics Corp. Fort Worth 1, Texas Attn: Mr. R. C. Chase Aerophysics Group Engineer THRU: Air Force Plant Representative CONVAIR P. O. Box 371 Fort Worth 1, Texas		

DISTRIBUTION LIST

<u>No. of Copies</u>	<u>Organization</u>	<u>No. of Copies</u>	<u>Organization</u>
1	Glenn L. Martin Company Middle River Baltimore 3, Maryland Attn: Mr. S. L. Rosing, Mail No. 356 THRU: Bureau of Aeronautics Rep. Glenn L. Martin Company Baltimore 3, Maryland	1	McDonnell Aircraft Corporation P. O. Box 516 St. Louis 3, Missouri Attn: Armament Group THRU: Bureau of Aeronautics Rep. McDonnell Aircraft Corp. St. Louis 3, Missouri
1	Grumman Aircraft Corporation Bethpage, Long Island, New York Attn: Armament Group THRU: Bureau of Aeronautics Rep. Grumman Aircraft Engineering Corporation Bethpage, Long Island, New York	1	Massachusetts Institute of Technology Building 23-111 Cambridge 39, Massachusetts Attn: Dr. James Mar THRU: Deputy District Chief Boston Ordnance District Boston Army Base Boston 10, Massachusetts
1	Hughes Aircraft Company Culver City, California Attn: Mr. Dana Johnson Research & Development Labs. THRU: Air Force Plant Rep., WEAPD Hughes Aircraft Company Florence Ave at Teal St. Culver City, California	1	Massachusetts Institute of Technology Room 41-219 Cambridge 39, Massachusetts Attn: Dr. Emmett A. Witmer THRU: Deputy District Chief Boston Ordnance District Boston Army Base Boston 10, Massachusetts
1	Institute for Cooperative Research Johns Hopkins University, Project THOR 3506 Greenway Baltimore 2, Maryland THRU: Deputy District Chief Baltimore Regional Office of the Phila Ord District Main Post Office Baltimore 1, Maryland	1	North American Aviation, Inc. 12214 Lakewood Blvd. Downey, California Attn: Mr. D. H. Mason Mr. J. Ward Engineering Technical File THRU: Air Force Plant Rep., WEAPD North American Aviation, Inc. Los Angeles International Airport Los Angeles 35, California
1	Lockheed Aircraft Corporation Military Operations Research Div. 1 Burbank, California Attn: Mr. R. A. Bailey, Div. Engineer THRU: Air Force Plant Rep., WEAPD Factory A Lockheed Aircraft Corporation Burbank, California		Northrop Aviation, Inc. Hawthorne, California Attn: H. K. Weiss THRU: Air Force Plant Rep., WEAPD Northrop Aviation, Inc. Hawthorne, California

DISTRIBUTION LIST

<u>No. of Copies</u>	<u>Organization</u>
2	Republic Aviation Corporation Farmingdale, Long Island, New York Attn: Armament Group Mr. M. Trauring, Plant No. 4 THRU: Air Force Plant Representative Republic Aviation Corporation Farmingdale, Long Island, New York
1	University of Chicago Institute for Air Weapons Research Museum of Science and Industry Chicago 37, Illinois Attn: Dr. David Saxon Mr. Herbert Hesse THRU: Commander Mid Central Air Procurement District 165 North Canal Street Chicago 15, Illinois
1	University of Pittsburgh Pittsburgh, Pennsylvania Attn: Mr. Malin THRU: Deputy District Chief Pittsburgh Ordnance District 200 4th Avenue Pittsburgh 22, Pennsylvania
1	Office, Asst. Secretary of Defense (R&D) Committee on Ordnance Washington 25, D. C.



AD-114 950

DEPARTMENT OF THE ARMY
UNITED STATES ARMY RESEARCH LABORATORY
ABERDEEN PROVING GROUND, MARYLAND 21005-5066

Rec'd
8/3/2000

REPLY TO
THE ATTENTION OF

AMSRL-CS-IO-SC (380)

28 July 2000

MEMORANDUM FOR Defense Technical Information Center, ATTN:
DTIC-BCS, 8725 John J. Kingman Road Suite 0944,
Ft. Belvoir, VA 22060-6218

SUBJECT: Distribution Statement for BRL Memorandum Report No.
1019

1. Reference: Ballistic Research Laboratories Memorandum Report
No. 1019, "Air Blast Measurements around Moving Explosive Charges,
Part III", by B. F. Armendt and J. Sperazza, July 1956.

2. The correct distribution statement for the referenced report
is:

Approved for public release; distribution is unlimited.

3. Request that you mark your copy of the report with this
distribution statement. Our action officer is Mr. Douglas J.
Kingsley, telephone 410-278-6960.

for Douglas Kingsley
BENJAMIN E. BRUSO
Team Leader, Security/CI Office

